ARTICLE IN PRESS
+ MODEL
Available online at www.sciencedirect.com
ScienceDirect
Environmental Modelling & Software xx (2007) 1–10
Environmental Modelling & Software
www.elsevier.com/locate/envsoft

A distributed model of water balance in the Motueka catchment, New Zealand

Robbie M. Andrew, John R. Dymond*

Landcare Research, Private Bag 11052, Palmerston North, New Zealand

Received 16 January 2006; received in revised form 30 August 2006; accepted 3 October 2006

Abstract

A distributed water balance model is used to simulate the soil moisture regime of the Motueka catchment. The model is a major simplification of the Distributed Hydrology–Vegetation–Soil Model (DHVSM) with modifications suitable for the study area. The model was applied at 25-m resolution with a 1-day time-step for 10 years. The simulated hydrograph showed good correspondence with the observed hydrograph and there was good agreement of simulated and measured mean annual discharges (57.3 $m^3 s^{-1}$ as compared with 58.7 $m^3 s^{-1}$). Five different land cover scenarios were used to predict the effects of vegetation change on the hydrological regime: (1) current land cover; (2) prehistoric land cover; (3) maximum pine planting; (4) pine trees on easy slopes; and (5) pine trees on steep slopes. The pine scenarios all reduced the mean annual flow by about 2 $m^3 s^{-1}$, while the prehistoric scenario reduced the mean annual flow by about 6 $m^3 s^{-1}$. The pine scenarios (3, 4, and 5) reduced the 7-day 5-year low flow from 7.4 $m^3 s^{-1}$ to between 6.5 $m^3 s^{-1}$ and 6.8 $m^3 s^{-1}$, respectively; and the prehistoric scenario reduced the 7-day 5-year low flow to 5.3 $m^3 s^{-1}$.

Keywords: Water balance model; Soil moisture regime; Simulation; Land cover scenarios; Hydrologic regime

1. Introduction

The Motueka catchment in the South Island of New Zealand has experienced major land use change over the last two centuries. When Europeans began migrating to the Nelson district in significant numbers around the 1840s, the land cover was primarily indigenous forest. Since then, most of the hill country and plains have been converted to pastoral agriculture; only the rugged mountains remain in indigenous forest. More recently, significant proportions of pastoral land have been planted in exotic pine trees (predominantly *Pinus radiata*). These changes in land use bring about significant changes in the hydrological regime, affecting the viability of various human activities. For example, increased planting of *P. radiata* reduces low flows of the Motueka River and the quantity of water available to horticulture during summer. Lower flows also increase the temperature and reduce the oxygen content of the water for fish, effectively reducing available fish habitat. The quantity of water and related water quality also have a major influence on the aquacultural industry in the coastal zone near the mouth of the Motueka River (Basher, 2003). Land use patterns also influence soil moisture regimes which control plant growth.

To help mediate between competing uses of water, it would be helpful to have a model that could evaluate the effects of land use pattern on the hydrological regime of the Motueka catchment, including both river flows and soil moisture patterns. As desktop computers increase in power, it is becoming more feasible to run distributed hydrology–vegetation models that model the spatial detail of the interaction between vegetation and hydrology. Croton and Bari (2001) discuss the development of distributed models and point out that, even though they are difficult to parameterise (Silberstein, 2005), distributed models are the only models that ''can describe the interplay between the multiple catchment attributes and processes, essential in understanding land use hydrology at the catchment scale''. And the requirement for spatially detailed parameters

* Corresponding author. Tel.: +64 6 3534955.
E-mail address: dymondj@landcareresearch.co.nz (J.R. Dymond).

1364-8152/$ - see front matter © 2006 Elsevier Ltd. All rights reserved.
doi:10.1016/j.envsoft.2006.10.006

Please cite this article in press as: Robbie M. Andrew, John R. Dymond, A distributed model of water balance in the Motueka catchment, New Zealand, Environ. Model. Softw. (2007), doi:10.1016/j.envsoft.2006.10.006

is partly being met by the development of remote sensing (Munro et al., 1998) and Geographic Information Systems (Pullar and Springer, 2000).

Wigmosta et al. (1994) developed a grid-based model of hydrology (DHVSM) that models most components of the hydrological cycle, that is, rainfall, interception, evapotranspiration, throughfall, percolation, groundwater flow, and runoff, at every grid point. Overland and river flows are not modelled spatially so that large time steps can be employed without incurring model instability: generated runoff is routed immediately to the catchment outlet. The grid-based model is compatible with raster data and so is directly able to use geographic information from raster GIS to control input parameters, such as climatic, soil hydraulic, and vegetative attributes. Model outputs, such as soil moisture and groundwater depth are also raster and easily manipulated and displayed with a raster GIS. DHVSM is convenient and can be used to model spatial complexity. However, there are a large number of computations per grid point, so model simulations of large catchments take a long time, even though time steps of several hours are employed.

In this paper, we describe a distributed vegetation–hydrology model similar to DHVSM, but much simplified to reduce execution time. We aimed to simplify the model sufficiently to speed up execution by an order of magnitude without compromising model accuracy. We plan to be able to run simulations of over 10 years with daily time steps for large catchments, like the Motueka (2200 km^2), at a spatial resolution of 25 m, overnight on our computer system (Sun UltraSparc III). We use the model to simulate the effect of several realistic land cover scenarios of the Motueka catchment on the hydrological regime: (1) prehistoric land cover; (2) current land cover; (3) maximum pine planting; (4) pine trees on steep land; and (5) pine trees on easy land. Although we simulate both soil moisture and river flows, we only test the accuracy of the model on the river flows, as comprehensive soil moisture measurements are unavailable.

2. Study area

The Motueka catchment comprises 2200 km^2 of land ranging from sea level to 1700 m in elevation. It is located in the northwest of the South Island of New Zealand (Fig. 1). The climate is temperate, with average annual precipitation ranging from 1200 mm at the coast to a maximum of 3000 mm in the west of the catchment. The mean annual runoff of the Motueka River is 844 mm (mean annual discharge is 58 $m^3 s^{-1}$at the Woodstock flow monitoring site). The river delivers 60% of the fresh water entering Tasman Bay, a productive and shallow coastal body of high cultural, economic, and ecological significance (Basher, 2003). There is a significant groundwater resource occurring in the terraces and floodplains of the upper Motueka (Basher, 2003).

Geology is mixed with clearly defined terrains that include erodible granites (mid-basin), clay-bound gravels (mid-basin), ultramafic mineral formation (eastern headwaters), sandstone–siltstone (eastern headwaters), and complex limestone, marble, and calcareous mudstone (western headwaters). Rolling and steep hill country in the lower basin contain low-fertility soils and are grazed or in plantation forest. The rugged mountainous terrains in the headwaters contain a mixture of thin-infertile to thick-fertile soils and are mostly in conservation estate. The part of the catchment to be modelled, which we call the study area, is upslope of the settlement of Woodstock (−41.24°S, 172.82°E; Fig. 2), where there is a long-term flow record for the river. The study area has 1800 km^2 of land, comprising 37% mixed indigenous forest, 27% plantation forest (*P. radiata*), 17% pasture, 10% scrub, 8% tussock, and 1% bare ground. Basher (2003) provides detailed metadata for the Motueka catchment.

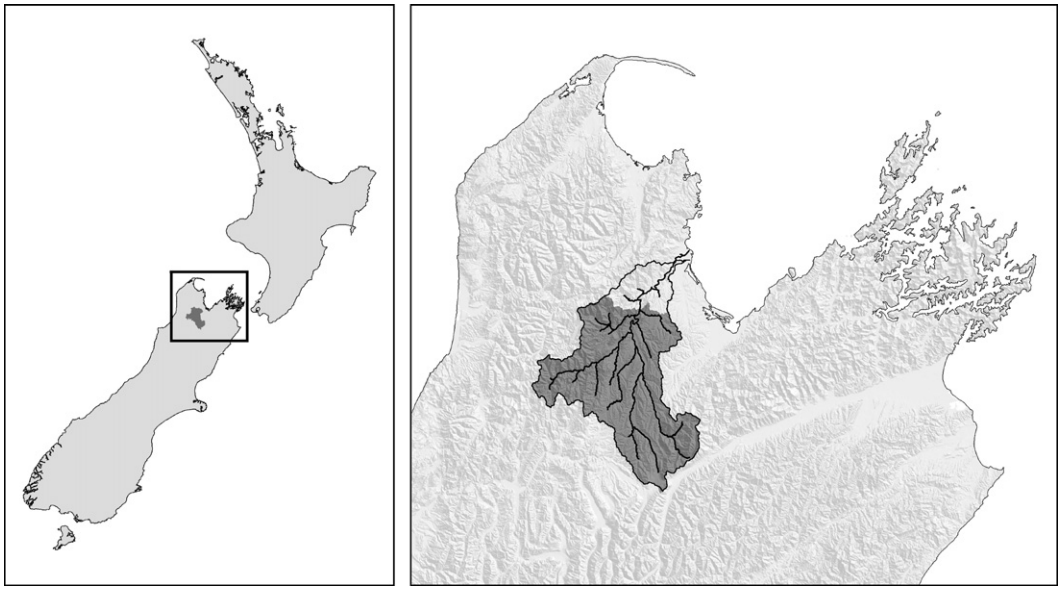

Fig. 1. Location of the study area: New Zealand (left) and the top of South Island (right).

Please cite this article in press as: Robbie M. Andrew, John R. Dymond, A distributed model of water balance in the Motueka catchment, New Zealand, Environ. Model. Softw. (2007), doi:10.1016/j.envsoft.2006.10.006

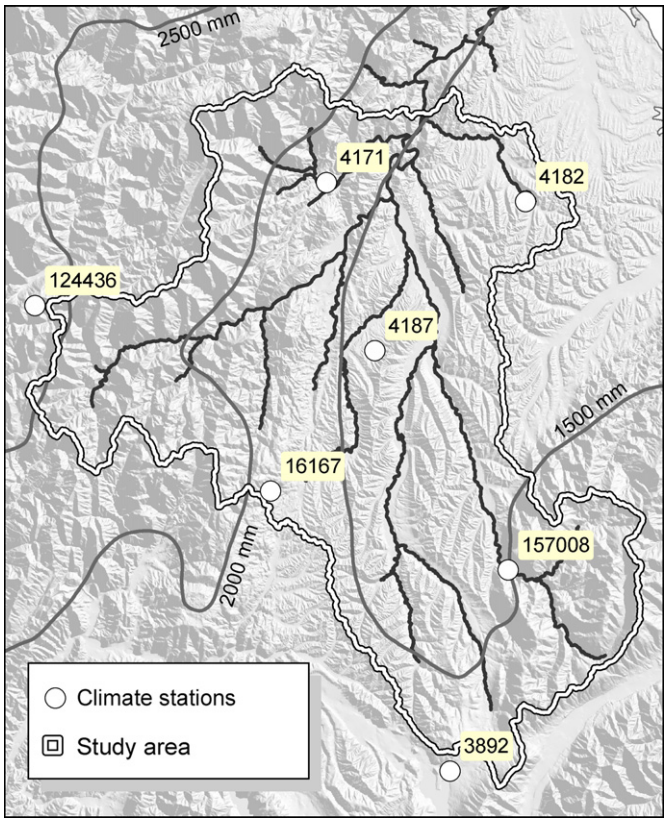

Fig. 2. Climate stations used in the rainfall interpolation procedure. Mean annual rainfall contours are given in mm.

2.1. Model development

The model comprises three main components: rainfall, evapotranspiration and water balance. As part of the water balance at each cell in a grid, it explicitly routes sub-surface flow between cells using surface elevation data.

2.2. Rainfall interpolation

As the main driver of the model, rainfall must be interpolated accurately over the study area. Rainfall in the Motueka catchment is highly dependent on elevation, so it was necessary to combine gauged rainfall at seven points with knowledge of how elevation influences rainfall. In a similar way to the method described by Lynch and Schultz (1995), we applied an inverse-distance–weight (Thornton et al., 1997) to estimates of rainfall from gauges: where the estimates are based on gauged rainfall and the ratio of mean annual rainfalls at the point to be predicted and at the gauge. Leathwick et al. (2002) derived the map of mean annual rainfall using the thin-plate spline method of Hutchinson (1995). Using mean annual rainfall ignores monthly variation in spatial relationships, but we accept this limitation as a first approximation.

A rainfall layer for each daily time-step is interpolated from daily rainfall read at the seven gauges. The interpolation is based on weighted averages with weights dependent on distance of the interpolated point from each gauge and the ratio of the gauge's annual rainfall to the annual rainfall at the interpolated point.

$$R(y) = \sum_j a_{y,x_j} b_{y,x_j} R(x_j) \tag{1}$$

where $a_{y,x_j} = g[D(y,x_j)] / \sum_i g[D(y,x_i)]$, $b_{y,x_j} = A(y)/A(x_j)$, $D(y,x_j)$ is the Euclidean distance between y and gauge j, and $g[\cdot]$ is the inverse squared-distance weighting function defined as $g[d] = 1/d^2$, $R(y)$ is the interpolated rainfall at y, $R(x_j)$ is the rainfall measured at gauge j, $A(y)$ is the mean annual rainfall at y, and $A(x_j)$ is the mean annual rainfall at gauge j.

A common method for validating interpolation is to make predictions at each gauge without using the gauge and compare against measurements. This method also has merit in estimating the sensitivity of the method to the inclusion/exclusion of individual stations. Results from validation over the 10-year period of study are shown for each station in Table 1. The interpolated surface for the study area is clearly very sensitive to gauges 124436 and 4187. Gauge 124436 at Wangapeka Saddle is the only data source representing the higher rainfall in the west of the study area, and gauge 4187 at Tadmor is the only centrally located gauge. The low sensitivity to data from gauge 16167 is beneficial because it contributes only 2½ years' worth of data.

2.3. Evapotranspiration

Precipitation is stored in the canopy up to a limit defined by the interception store capacity. At the start of each simulated day all contents of the interception store are evaporated as the daily evaporation always exceeds the capacity of the interception store. Transpiration is estimated as a fraction of the potential evapotranspiration. Transpiration draws water first from the unsaturated store, and then from the saturated store if required to fill the quota. Neither snowfall nor evaporation directly from the soil surface has been included in the model, as they generally make small contributions to the hydrological cycle in the Motueka catchment.

Wigmosta et al. (1994) showed that the ratio of actual to potential evapotranspiration (PE) is,

$$\frac{E_a}{E_p} = \frac{\Delta + \gamma}{\Delta + \gamma(1 + r_c/r_a)} \tag{2}$$

Table 1
Jack-knifing results for the rainfall interpolation method, showing totals, root-mean-square errors (RMSE), mean absolute errors (MAE), and bias

Gauge station	Days	Total measured (mm)	Total predicted (mm)	RMSE	MAE	Bias (%)
16167	852	4083	3949	0.46	0.20	−3.28
4171	3189	14 514	13 923	0.53	0.23	−4.07
4187	3351	10 179	12 621	0.40	0.17	23.99
4182	3238	9890	10 191	0.46	0.19	3.05
157008	3551	11 684	11 882	0.57	0.25	1.69
3892	3592	15 647	15 204	0.70	0.30	−2.83
124436	3652	40 921	28 879	2.07	0.97	−29.43

Please cite this article in press as: Robbie M. Andrew, John R. Dymond, A distributed model of water balance in the Motueka catchment, New Zealand, Environ. Model. Softw. (2007), doi:10.1016/j.envsoft.2006.10.006

where E_a is the rate of transpiration from vegetation with a dry surface, E_p is the rate from wet surfaces, Δ is the slope of the saturated vapour pressure–temperature curve, γ is the psychrometer constant, r_c is the canopy resistance to vapour transport, and r_a is the aerodynamic resistance to vapour transport. Values used for r_c and r_a are vegetation-dependent (see Table 2) and are assumed constant, unlike Wigmosta et al. (1994) who permitted variation with leaf area index (LAI). However, soil moisture limitation is modelled similarly to Wigmosta et al. (1994) and is thought to dominate any variation of canopy resistance with LAI:

$$r_c = \begin{cases} \frac{\theta_r - \theta_m}{\theta - \theta_m} r_{c(\min)} & \text{if } \theta \le \theta_r \\ r_{c(\min)} & \text{if } \theta > \theta_r \end{cases} \quad (3)$$

where θ is the current soil moisture, θ_r is field capacity, θ_m is wilting point, and $r_{c(\min)}$ is the canopy resistance at field capacity. If available water $(\theta - \theta_m)$ is zero, transpiration is bypassed. It is possible that during drought conditions, canopy resistance may vary with leaf biomass, however, the soil moisture limitation will dominate this.

The psychrometer constant, γ, and slope of the saturated vapour pressure–temperature curve, Δ, are both temperature dependent (Jones, 1992; Allen et al., 1998) and need to be estimated for each daily simulation. The daylight mean temperature can be calculated from the maximum and minimum temperatures using the formula given by Goudriaan and Van Laar (1994):

$$T_{day} = 0.71T_{max} + 0.29T_{min} \quad (4)$$

To estimate daily temperature over the catchment we use daily maximum and minimum temperatures from the Appleby meteorological site (25 km NE of Woodstock) and an adiabatic lapse rate to adjust for elevation. Our analysis of temperature data within the catchment indicated an ALR of 6.0 °C/km.

The potential evapotranspiration data used were calculated as long-term monthly average surfaces using the FAO-Penman method (Allen et al., 1998) for the standard grass crop (these monthly average PE surfaces were calculated by Leathwick et al. (2002) for all New Zealand). These data need to be adjusted for other vegetation types based on a vegetation factor, K_{veg}, which we have calculated as monthly averages from daily climate data using a full Penman–Monteith calculation of a whole year of data. The actual evapotranspiration (conditional on availability of water) then becomes:

Table 2
Vegetative land cover classes present in the study area, and their assigned canopy and aerodynamic resistances, and canopy interception capacities (from data given by Fahey, 2002 and Fahey and Rowe, 1992)

Land cover	Area (%)	r_a	$r_{c(min)}$	$S_{i:max}$ (mm)
Pasture	17	30	50	0.7
Native forest	37	6.5	140	1.9
Planted forest	27	6.5	112	1.3
Scrub	10	6.5	160	2.0
Tussock	8	7.0	120	0.6

$$E_a = (K_{veg}E_p)\frac{\Delta + \gamma}{\Delta + \gamma(1 + r_c/r_a)} \quad (5)$$

2.4. Water balance

The water balance in each cell is simulated by two reservoirs (Fig. 3) corresponding to the canopy interception store (S_i) and the soil column. The water depth in the soil column is separated into a saturated component (S_s) and an unsaturated component (S_u), which the model calculates at time steps of interval Δt. These two components are a simplification of the DHVSM which has three components: upper rooting zone, lower rooting zone, and saturated zone.

At each time-step, all water in the interception store (S_i) is evaporated. Transpiration (E_s) is calculated as:

$$E_s = \min(E_a, S_s + S_u) \quad (6)$$

where E_a is given by Eq. (5).

To obtain a daily interception capacity from the instantaneous capacity ($S_{i:max}$), the instantaneous capacity is scaled by $F_{veg} = 1.33$ to account for multiple evaporative cycles throughout the day (the factor of 1.33 brought the total evaporative loss from 300 mm/yr up to 400 mm/yr as expected by Fahey and Rowe (1992)). The rainfall interception (P_i) is then calculated from the rainfall input (P) as:

$$P_i = \min(P, F_{veg}S_{i:max}) \quad (7)$$

The water balance of the unsaturated component of soil water is calculated similarly to Wigmosta et al. (1994), except that Hortonian overland flow is permitted. Throughfall is split between infiltration (P_s) and surface runoff according to the current balance of the soil column and the maximum infiltration rate ($P_{s:max}$), estimated from saturated hydraulic conductivity, K_{sat}. When the soil column is full, there is saturated overland flow, R_{sat}. When throughfall exceeds the maximum infiltration rate, there is Hortonian overland flow, R_{Hort}.

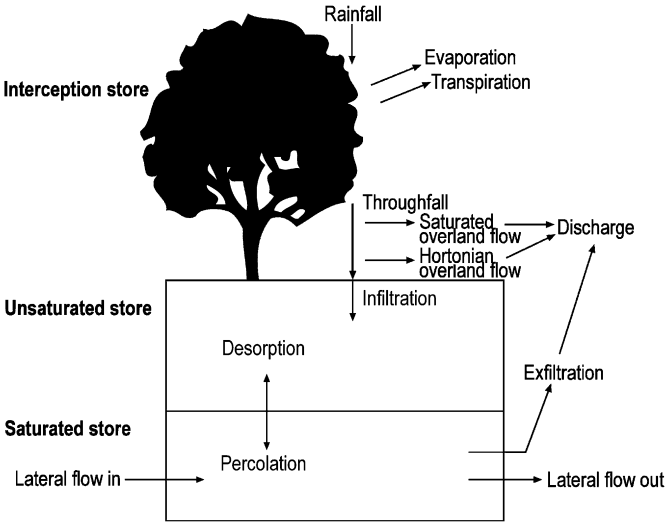

Fig. 3. Structure of the model.

Please cite this article in press as: Robbie M. Andrew, John R. Dymond, A distributed model of water balance in the Motueka catchment, New Zealand, Environ. Model. Softw. (2007), doi:10.1016/j.envsoft.2006.10.006

$$P_{s:max} = K_{sat}\Delta t \tag{8}$$

$$R_{Hort} = \max(0, P - P_i - P_{s:max}) \tag{9}$$

$$R_{sat} = \max(0, P - P_i - R_{Hort} - (S_{s:max} - (S_s + S_u))) \tag{10}$$

$$P_s = P - P_i - R_{Hort} - R_{sat} \tag{11}$$

Following Wigmosta et al. (1994), lateral sub-surface flow velocity (v) from the saturated component of the soil column is calculated from Darcy's equation using the surface slope in the direction of flow (s), and assuming a constant K_{sat} down the soil profile:

$$v = K_{sat}\sin(s) \tag{12}$$

The volume of water removed from the soil column (Q_{lat}) is then given by,

$$Q_{lat} = vd\Delta t\frac{S_s}{0.5} \tag{13}$$

$$Q_{lat} = \min\left(vd\Delta t\frac{S_s}{0.5}, S_s + S_u - \theta_r\right) \tag{14}$$

where Δt is the time-step, d is the cell width, and $S_s/0.5$ is the effective depth of the saturated component of the soil column assuming 50% porosity. Lateral sub-surface flow is added to the down-slope cell, based on an eight-connected neighbourhood (calculated using the *Flowdirection* function in Arc Grid (ESRI, 1991)). If a down-slope cell becomes saturated as a result of lateral inflow, the excess (Q_{ex}) is exfiltrated.

Surface runoff at time-step n from cell p (Q_p^n) is calculated as:

$$Q_p^n = R_{sat} + R_{Hort} + Q_{ex} \tag{15}$$

There is no explicit routing of surface runoff in the model. All surface runoff is sent via a delay function to the catchment mouth. To approximate the surface-flow recession curve of the catchment, a 1-day delay function is applied to the discharge, so that the catchment discharge at time-step n (Q^n) is given by,

$$Q^n = 0.67\sum_p Q_p^n + 0.33\sum_p Q_p^{n-1} \tag{16}$$

We have simplified the percolation and desorption components of DHVSM to a rapid balance between the saturated and unsaturated components of water in the soil column:

1. if the soil column is at maximum capacity, the unsaturated component is set to zero to represent saturation;
2. if the unsaturated component is greater than field capacity, the excess is percolated to the saturated component at the maximum infiltration rate;
3. if the unsaturated store is lower than half of field capacity, then the difference ($0.5FC - S_u$) is made up from the saturated store instantaneously. This effectively models desorption discretely whenever half of field capacity is reached; and
4. if the soil column was at maximum capacity, and is no longer, a fraction of the quantity lost is transferred from the saturated store to the unsaturated store. This occurs following transpiration and lateral flow.

3. Input data

3.1. Land cover

Land cover data were taken from the NZ Land Cover Database (MfE, 2000). There are 16 land cover classes in the classification scheme, of which eight are vegetative, and five are present at greater than 0.1% of the study area. These five vegetative covers have been assigned canopy-to-aerodynamic resistance ratios for use in the calculation of evapotranspiration, and interception store capacities, based on data averaged from Fahey (2002), and shown in Table 2. The three remaining vegetative cover classes (horticulture, riparian willows and mangroves) each represent less than 0.05% of the study area and have been assigned the same parameters as pasture.

3.2. Digital elevation model

Digital elevation data were taken from a New Zealand 25 m DEM, interpolated from the national 20 m contour set (Barringer and Lilburne, 1997). Dymond and Harmsworth (1994) considered 12.5 m DEMs were necessary to capture most topographic detail of New Zealand landscapes from 20 m contours, but we opted for 25 m to keep processing time down. Cell sizes greater than 25 m would be inappropriate as there are significant differences in soil moisture over distances of 100 m in the Motueka. Topographic sinks (depressions) in the DEM were filled to allow unrestricted flow of water to the catchment mouth.

3.3. Climate data

Mean annual rainfall and mean monthly potential evapotranspiration were taken from the Land Environments New Zealand database (Leathwick et al., 2002), where evapotranspiration is calculated using Penman–Monteith (Allen et al., 1998) with long-term monthly averages. Because these climate data were continuous and relatively slowly varying, they were input at one-tenth the spatial resolution of the other data to reduce storage and computation time. Daily rainfall data for the period 1990–1999 were taken from the NIWA Climate Database (CLIDB; Penney, 2001) and Tasman District Council's records. Data from seven stations were used in the rainfall interpolation process (Fig. 2).

3.4. Soil properties

Soil properties for the study area were extracted from the Fundamental Data Layers (Newsome et al., 2000), which are a series of digital national maps of soil characteristics produced from a combination of expert knowledge and soil sampling/mapping. The water-holding capacity of the soil is

Please cite this article in press as: Robbie M. Andrew, John R. Dymond, A distributed model of water balance in the Motueka catchment, New Zealand, Environ. Model. Softw. (2007), doi:10.1016/j.envsoft.2006.10.006

defined for each grid cell by three quantities: field capacity (θ_r), wilting point (θ_m), and the total capacity (θ_T). For the purposes of the model, wilting point is treated as a lower limit, so water contents are expressed relative to wilting point. Field capacity and total capacity are calculated by,

$$\theta_r = \theta_m + \text{PAW\_MID}$$

$$\theta_T = \theta_r + \text{MPOR\_MID}$$

where PAW_MID is the middle of the expected range of ''profile total available water'' (the water held in the soil between tensions of −10 kPa and −1500 kPa) and MPOR_MID is the middle of the expected range of ''macroporosity'' (the water held in the soil between saturation and −10 kPa).

Saturated hydraulic conductivity (K_{sat}), used as an approximation of actual hydraulic conductivity, was taken from the ''Permeability Profile'' field of the Fundamental Data Layers. The permeability profile gives only a very coarse description of permeability (rapid, medium, or slow). K_{sat} varied with soil type but was held constant for the soil depth. If two permeability layers were present in the profile then the deeper of the two permeability values was taken. The textual codes were converted to conductivities as shown in Table 3.

3.5. Soil moisture initialisation

Saturating the soil everywhere and then running the model for 40 days with no rain initialised the soil moisture over the catchment. This method gives empty canopy interception stores, which is reasonable given the mid-summer start of the simulation period. The resulting spatial water balance was used as the initial state for all simulations.

4. Model calibration

Saturated hydraulic conductivity (K_{sat}) for Darcy flow (i.e. the lateral component) was estimated by calibrating the simulated hydrograph to best match the measured hydrograph at Woodstock. We varied K_{sat} for Darcy flow by scaling the values from the GIS layer with a catchment-wide constant, while the vertical component of K_{sat} remained set by the GIS layer. K_{sat} for Darcy flow is recognised as being a difficult parameter to quantify because of its high spatial variability, and the data for the Motueka catchment are based on very few point samples. The scaling constant was chosen to minimise the mean square error (MSE) for the 1992 hydrograph:

$$\text{MSE} = \frac{1}{|I_t|}\sum_{i\in I_t}\left(Q_i - \widehat{Q}_i\right)^2 \tag{17}$$

where Q_i and $\widehat{Q}_i$ are measured and simulated flow at time i, respectively, $I_t = \{i : Q_i < Q_t\}$ and Q_t was set at 100 $m^3 s^{-1}$ − a threshold chosen to exclude peaks which have larger absolute errors. The scale factor that minimised this error term was 250, so K_{sat} for Darcy flow was scaled by a factor of 250 compared with the values given in Table 3. A visual comparison of hydrographs confirmed that this scaling factor gave the best results. Such a large factor is due to scale differences in K_{sat}: at the field scale (~100 m) K_{sat} must take into account preferential flowpaths (Deurer et al., 2003).

4.1. Hydrograph post-processing

Because the model does not represent movement of water to and from aquifers, simulated low flows are often lower than those observed. On a cell-by-cell basis this represents a small error, and the spatial pattern of soil moisture is not greatly affected, but the hydrograph accumulates these errors. Rather than correct for aquifers at a cell level, we introduce a simple post-processing model that effectively redirects a proportion of surface flow to aquifer flow, spread over a period of 90 days.

A normalised convolution kernel is used to redistribute flow through time, and is defined as:

$$k(i) = \frac{1+\cos(\pi i/N)}{\sum_{j=1}^{N}[1+\cos(\pi j/N)]} \tag{18}$$

where we have used $N = 90$ days. The adjusted hydrograph, Q', is then calculated from the raw hydrograph, Q, using the following equation:

$$Q' = (1-a)Q + aQ \otimes k \tag{19}$$

where a is the fraction of surface flow water to redistribute as base flow, and $\otimes$ is the convolution operator. The cosine function provides a weighting of the redistribution such that base flow from recent days contributes more than does base flow from earlier days, with a slowly varying weight in between. We used a value of $a = 0.3$, causing 30% of the surface flow to be delayed and temporally redistributed as base flow. N and a were found by mean-square-error minimisation. The value of a is within the measured range of the Moutere catchments, near Nelson (Rowe et al., 2002).

5. Land cover scenarios

In addition to the current land cover, four further scenarios were simulated to examine the effects of land use change on the hydrological regime. An inferred ''prehistoric'' (before human colonisation) land cover scenario was taken from the Land Environments New Zealand classification (LENZ; Leathwick et al., 2002). These data show the catchment as being 90% forest and 10% scrub.

Table 3
Permeability codes from the Fundamental Data Layers database and the hydraulic conductivities assigned to them (following Griffiths, 1985)

Permeability code	Conductivity range (mm/h)	Value used (mm/h)
Slow	<4	3
Moderate	4–72	40
Rapid	>72	120

Please cite this article in press as: Robbie M. Andrew, John R. Dymond, A distributed model of water balance in the Motueka catchment, New Zealand, Environ. Model. Softw. (2007), doi:10.1016/j.envsoft.2006.10.006

A "maximum pine" scenario was created to reflect the importance of the conversion of pasture and scrub to *P. radiata* plantations. *P. radiata* is the dominant species found in plantation forests in New Zealand, accounting for 89% of the plantation estate (New Zealand Forest Owners Association, 2002). The intention of the maximum pine scenario was to represent the maximum possible extent of pine plantations in the catchment, based on both physiological and financial limitations to its growth, and reflecting the fact that areas of indigenous forest, protected by government charter, are unlikely to be planted in plantation pine. Areas excluded from pines in the maximum pine scenario were ultramafic areas in the southeast of the catchment, high country above 600 m, urban and horticultural areas, and indigenous forest and wetlands.

Two further scenarios were created to study the effect of pine plantation distribution within the study area. The areas available were limited to those of the "maximum pine" scenario, with the additional exclusion of scrub areas so that only the effect of conversion from pasture to pine was present. The area then available for pine was divided into two approximately equal areas, based on a slope threshold of 15°. This produced two land cover scenarios: "pine on steep slopes" and "pine on easy slopes". Table 4 summarises the areas of the vegetation classes in the five scenarios.

Table 4
Areas of the vegetation classes in the five land cover scenarios

Land cover	Current land cover (%)	Prehistoric land cover (%)	Maximum pines (%)	Pines on steep slopes (%)	Pines on easy slopes (%)
Indigenous forest	37	90	37	37	37
Pine forest	27	0	49	34	34
Pasture	17	0	1	10	10
Scrub	10	10	4	10	10
Tussock	8	0	7	8	8

6. Results

The model was run for a period of 10 years (1990–1999) with a daily time-step and a 25×25 m cell resolution, amounting to 2.8 million calculations per time-step, or 10.2 billion per simulation. The daily time-step is large to keep the total number of calculations low, but it is still smaller than the time for significant action to occur in the base flow. For each day the daily soil moisture pattern is simulated as well as the daily discharge. These spatial outputs are not discarded and are available for analysis over the entire simulation period, but we do not present these results here. For the current land cover scenario, the simulated hydrograph, after calibration, compared well with the observed hydrograph. The 1998 calendar year, shown in Fig. 4, had several large-magnitude storm events, including a cluster in October and early November, and these are well represented by the model. Peaks in the simulated discharge coincide closely in time with those of the observation record. Some peaks are over-estimated, but this is more likely a failing of the rainfall interpolation than of the water balance model. There are instances in other simulated years (not shown here) of summer storm events with simulated peaks far in excess of those in the observation record. Examination of the rainfall station data at these times indicates that the storms in question were probably localised, but the interpolation procedure effectively assumes that storm events occur over the whole catchment. Total annual discharges from the simulation of current land cover compare favourably with those of the observations (Fig. 5).

The model was run on the four alternative land cover scenarios to determine the impact of potential land use change on the hydrological regime of the Motueka catchment. The model simulation for the 10-year period, with current land cover, had a mean annual flow of 57.3 $m^3 s^{-1}$, which compares well with the annual flow of 58.7 $m^3 s^{-1}$ from the observations over the same period (Table 5; the long-term mean annual flow at Woodstock is 58.1 $m^3 s^{-1}$). The annual flow for the prehistoric scenario was lower at 51.1 $m^3 s^{-1}$, while the annual flows of the three pine scenarios were all about the same at 55 $m^3 s^{-1}$.

The hydrograph post-processing raised the low-flow levels by temporally redistributing surface flow over a period of 90 days. Fig. 6 shows the improvement of low flows caused by the post-processing model, with no appreciable effect at higher flow rates.

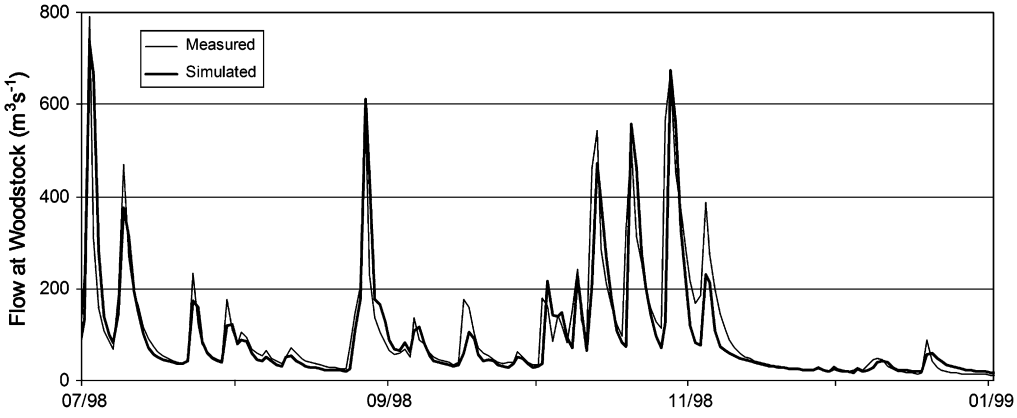

Fig. 4. Observed and simulated hydrographs for 1998.

Please cite this article in press as: Robbie M. Andrew, John R. Dymond, A distributed model of water balance in the Motueka catchment, New Zealand, Environ. Model. Softw. (2007), doi:10.1016/j.envsoft.2006.10.006

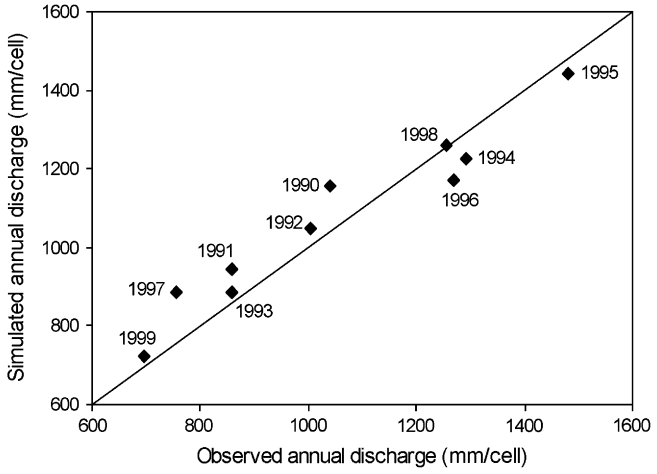

Fig. 5. Comparison of annual discharge totals between observations and simulations based on current land cover.

The measured 7-day, 5-year low flow of the Motueka River (1969–2001) is 7.4 $m^3 s^{-1}$, calculated using Weibull plotting positions. Because the duration of the simulation is only 10 years, it would be inappropriate to use Weibull plotting positions to calculate low flows from the simulated hydrographs. Instead, we fit a LOESS (locally weighted regression) model to the relationship between the discharges from the current scenario and those of the alternative scenarios. We used this regression model to predict the scenario low flow from the measured value of 7.4 $m^3 s^{-1}$. The LOESS model ensures that the regression fit to low flows is not affected by the fit to high flows. The results shown in Table 5 were calculated from post-processed hydrographs (the same calculations performed on the raw hydrographs gave results within 0.5% of those shown here). The estimated 7-day, 5-year low flow for the prehistoric land cover scenario was markedly lower (5.3 $m^3 s^{-1}$) than the long-term value of 7.4 $m^3 s^{-1}$. The values for the three pine scenarios were also lower than the observed record, ranging between 6.5 $m^3 s^{-1}$ and 6.8 $m^3 s^{-1}$.

7. Discussion

Based on information given by Whitaker et al. (2003), who applied the Distributed Hydrology–Vegetation–Soil Model of Wigmosta et al. (1994), we calculated the processing time of the model described here to be approximately an order of magnitude faster than the DHSVM. The extra speed is primarily brought about by three simplifications: (i) the soil water zone is reduced from three to two components; (ii) percolation and desorption are modelled by a rapid water balance between the two components of the soil water zone; and (iii) the overstory and understory canopy, and soil surface are all replaced by a single canopy (when bare ground is common, soil evaporation would have to be included). This enables the processing of simulations of large catchments (in the order of 2000 km^2) overnight. Although the reduction of complexity has created a model that runs much faster, it still produces accurate hydrograph shapes and magnitudes. Given the speed and apparent accuracy of the model, the simulation of effects of land cover change over large areas becomes possible. For very large catchments where water takes many days to reach the outlet, then a routing scheme that accounts for position in the catchment would be required.

The five land cover scenarios demonstrated that forests produce on average less runoff and lower low flows than

Table 5
Annual discharges and 7-day 5-year low flows from observations and simulated scenarios, 1990–1999

Hydrograph	Annual flow ($m^3 s^{-1}$)	Estimated 7-day, 5-year low flow ($m^3 s^{-1}$)
Observed	58.7	7.4
Current scenario	57.3	7.4
Prehistoric scenario	51.1	5.3
Maximum pine scenario	55.4	6.7
Pine on easy slopes scenario	55.2	6.5
Pine on steep slopes scenario	55.4	6.8

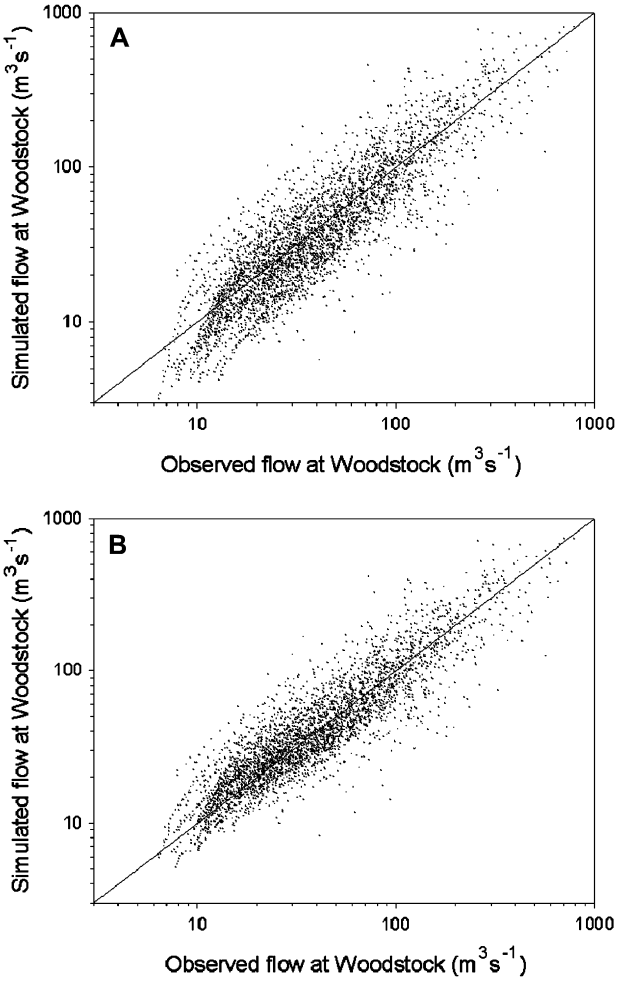

Fig. 6. Simulated flow compared with observed flow at Woodstock: (a) raw flow from model, and (b) flow post-processed to correct low flows.

Please cite this article in press as: Robbie M. Andrew, John R. Dymond, A distributed model of water balance in the Motueka catchment, New Zealand, Environ. Model. Softw. (2007), doi:10.1016/j.envsoft.2006.10.006

pasture. This is consistent with Rowe et al. (2002) who concluded from published data of paired catchments that both pine and indigenous forest have about 70% of the runoff from pasture. The reduction in runoff and low flows is caused by the higher average evapotranspiration of forests. Given that transpiration of forests in our model is lower than that of pastures, because pastures have a very high aerodynamic resistance, it is the evaporation of trees, through a greater interception store that controls the extra water usage. The three pine scenarios produced similar results for average runoff production and low flows. This does not necessarily imply trees on steep slopes produce the same runoff as trees on easy slopes, as much of the catchment is already in pine on a range of slopes. What it does imply is that pursuing a policy, from now on, of planting trees either on steep or easy slopes will have little effect on average runoff production or low flows.

We have developed a simplified, fast, distributed soil hydrology model that is accurate at the large catchment scale. The most difficult aspect of the model is obtaining sufficiently accurate input data. Rainfall is critical and requires a network of raingauges that is sufficiently dense. We have already mentioned the deficiency of potential evaporation, and accurate soil information over large areas is expensive to obtain. However, if data are available, calibration is straightforward, with only three parameters to estimate. The model is accurate for simulating discharge. However, it has not yet been tested for simulation of soil moisture patterns, which must wait for the ability to map soil moisture patterns over large areas.

8. Conclusions

The model presented in this paper is a simplification of a typical distributed hydrological model which attempts to represent all known hydrological processes with full spatial variation. The simplification improves speed by an order of magnitude while retaining acceptable accuracy of measured discharge. The increase of speed permits simulations of large catchments and the evaluation of land cover scenarios over large catchment scales. The model is useful for evaluating the effect of land cover scenarios on discharge, and is potentially useful for evaluating the effect of land cover scenarios on soil moisture regimes. Simulations of the Motueka catchment, in the Tasman District of New Zealand, show that planting of trees on steep or easy slopes will have little effect on average discharge or low flows.

Acknowledgments

Barry Fahey provided information on the resistance terms for the evapotranspiration calculation and helped develop the pine land cover scenarios. Hugh Wilde and Janice Willoughby assisted with soils data. John Leathwick provided data and information on long-term potential evapotranspiration averages. Tim Davie and Andrew Fenemor provided useful comments on the manuscript. Breck Bowden provided ideas about land cover scenarios, Rick Jackson provided assistance with water balancing, and Les Basher provided useful comments on model structure. The Tasman District Council provided meteorological data. This work was funded through Foundation for Research Science and Technology contract C09X0214 as part of a multidisciplinary research programme (visit the website at http://icm.landcareresearch.co.nz).

References

Allen, R., Pereira, L.S., Raes, D., Smith, M., 1998. Crop evapotranspiration – guidelines for computing crop water requirements. FAO Irrigation and Drainage Paper 56. Available from: http://www.fao.org/docrep/X0490E/x0490e00.htm.

Barringer, J., Lilburne, L., 1997. An evaluation of digital elevation models for upgrading New Zealand Land Resource Inventory slope data. In: Proceedings of Geocomputation 97. University of Otago, Dunedin, New Zealand, pp. 109–116.

Basher, L.R., 2003. The Motueka and Riwaka Catchments. Landcare Research, Lincoln, New Zealand.

Croton, J.T., Bari, M.A., 2001. Using WEC-C, a distributed, deterministic catchment model, to simulate hydrologic responses to agricultural clearing. Environmental Modelling & Software 16, 601–614.

Deurer, M., Green, S.R., Clothier, B.E., Bottcher, J., Duijnisveld, W.H.M., 2003. Drainage networks in soils. A concept to describe bypass-flow pathways. Journal of Hydrology 272, 148–162.

Dymond, J.R., Harmsworth, G.R., 1994. Towards automated land resource mapping using digital terrain models. ITC Journal 1994-2, 129–138.

Environmental Systems Research Institute, 1991. Cell-based modeling with GRID. In: ARC/INFO User's Guide, vol. 6. ESRI, Redlands, CA.

Fahey, B.D., 2002. Canopy Storage Capacities, and Aerodynamic Resistance and Canopy Resistance Values for Selected Species and Common Vegetation Types in New Zealand. Unpublished Report. Landcare Research, Lincoln, New Zealand.

Fahey, B.D., Rowe, L.K., 1992. Land-use impacts. In: Mosley, M.P. (Ed.), Waters of New Zealand. New Zealand Hydrological Society, Wellington.

Goudriaan, J., Van Laar, H.H., 1994. Modelling Potential Crop Growth Processes: Textbook with Exercises. Kluwer Academic Publishers, Dordrecht.

Griffiths, E., 1985. Interpretation of Soil Morphology for Assessing Moisture Movement and Storage. New Zealand Soil Bureau, Scientific Report 74. Department of Scientific and Industrial Research, Lower Hutt.

Hutchinson, M.F., 1995. Interpolating mean rainfall using thin plate smoothing splines. International Journal of Geographical Information Systems 9, 385–403.

Jones, H.G., 1992. Plants and Microclimate, second ed. Cambridge University Press.

Leathwick, J., Morgan, F., Wilson, G., Rutledge, D., McLeod, M., 2002. Land Environments of New Zealand: A Technical Guide. Ministry for the Environment, Wellington, New Zealand.

Lynch, S.D., Schultz, R.E., 1995. Techniques for estimating areal daily rainfall. In: Proceedings of the 15th Annual ESRI User Conference, Palm Springs, CA, USA.

Ministry for the Environment, 2000. New Zealand Land Cover Database. Ministry for the Environment, Wellington, New Zealand.

Munro, R.K., Lyons, W.F., Shao, Y., Wood, M.S., Hood, L.M., Leslie, L.M., 1998. Modelling land surface–atmosphere interactions over the Australian continent with an emphasis on the role of soil moisture. Environmental Modelling & Software 13, 333–339.

New Zealand Forest Owners Association, 2002. NZ Forest Industry Facts & Figures 2002/2003. Available from: <http://www.nzfoa.org.nz/file_libraries/facts_figures>.

Newsome, P.F.J., Wilde, R.H., Willoughby, E.J., 2000. Land Resource Information System Spatial Data Layers. Unpublished Report. Landcare Research, Lincoln, New Zealand.

Please cite this article in press as: Robbie M. Andrew, John R. Dymond, A distributed model of water balance in the Motueka catchment, New Zealand, Environ. Model. Softw. (2007), doi:10.1016/j.envsoft.2006.10.006

Penney, A.C., 2001. Climate Database (CLIDB) User's Manual. NIWA Technical Report 105, fifth ed. NIWA, Wellington.

Pullar, D., Springer, D., 2000. Towards integrating GIS and catchment models. Environmental Modelling & Software 15, 451–459.

Rowe, L., Jackson, R., Fahey, B., 2002. Land use and Water Resources: Hydrological Effects of Different Vegetation Covers. Landcare Research Contract Report: LC0203/027. Landcare Research, Lincoln, New Zealand.

Silberstein, R.P., 2005. Hydrological models are so good, do we still need data? Environmental Modelling & Software 21, 1340–1352.

Thornton, P.E., Running, S.W., White, M.A., 1997. Generating surfaces of daily meteorological variables over large regions of complex terrain. Journal of Hydrology 190, 214–251.

Whitaker, A., Alila, Y., Beckers, J., Toews, D., 2003. Application of the Distributed Hydrology Soil Vegetation Model to Redfish Creek, British Columbia: model evaluation using internal catchment data. Hydrological Processes 17, 199–224.

Wigmosta, M.S., Vail, L.W., Lettenmaier, D.P., 1994. A distributed hydrology–vegetation model for complex terrain. Water Resources Research 30, 1665–1679.

Please cite this article in press as: Robbie M. Andrew, John R. Dymond, A distributed model of water balance in the Motueka catchment, New Zealand, Environ. Model. Softw. (2007), doi:10.1016/j.envsoft.2006.10.006